Journal of Environmental Radioactivity 153 (2016) 156–166

Contents lists available at ScienceDirect

Journal of Environmental Radioactivity

journal homepage: www.elsevier.com/locate/jenvrad

Role of natural organic matter on iodine and ^{239,240}Pu distribution and mobility in environmental samples from the northwestern Fukushima Prefecture, Japan

Chen Xu [a, *], Saijin Zhang [a], Yuko Sugiyama [b], Nobuhito Ohte [c], Yi-Fang Ho [a], Nobuhide Fujitake [d], Daniel I. Kaplan [e], Chris M. Yeager [f], Kathleen Schwehr [a], Peter H. Santschi [a]

[a] Laboratory for Environmental and Oceanographic Research, Department of Marine Sciences, Texas A&M University, Building 3029, Galveston, TX, 77551, USA
[b] School of Human Science and Environment, University of Hyogo, 1-1-12 Shinzaike-Honcho, Himeji, Hyogo, 670-0092, Japan
[c] Department of Social Informatics, Graduate School of Informatics, Kyoto University, Kyoto, 606-8501, Japan
[d] Division of Agroenvironmental Biology, Graduate School of Agriculture Science, Kobe University, 1-1 Rokkodai, Nada-ku, Kobe, 657-8501, Japan
[e] Savannah River National Laboratory, Aiken, SC, 29808, USA
[f] Los Alamos National Laboratory, Los Alamos, NM, 87545, USA

ARTICLE INFO

Article history:
Received 25 August 2015
Received in revised form
23 December 2015
Accepted 27 December 2015
Available online xxx

Keywords:
Fukushima Prefecture
Iodine
Iodide
Iodate
Organo-iodine
Speciation
Plutonium
Isotopic ratio
Cesium
pH
Eh
Soil organic matter (SOM)
Nitrogen-containing organic compounds
Deciduous forest
Coniferous forest
Urban
Paddy
Stemwater
Throughfall
Bulk deposition

ABSTRACT

In order to assess how environmental factors are affecting the distribution and migration of radioiodine and plutonium that were emitted from the Fukushima Dai-ichi Nuclear Power Plant (FDNPP) accident, we quantified iodine and ^{239,240}Pu concentration changes in soil samples with different land uses (urban, paddy, deciduous forest and coniferous forest), as well as iodine speciation in surface water and rainwater. Sampling locations were 53–63 km northwest of the FDNPP within a 75-km radius, in close proximity of each other. A ranking of the land uses by their surface soil (<4 cm) stable ^{127}I concentrations was coniferous forest > deciduous forest > urban > paddy, and ^{239,240}Pu concentrations ranked as deciduous forest > coniferous forest > paddy ≥ urban. Both were quite distinct from that of ^{134}Cs and ^{137}Cs: urban > coniferous forest > deciduous forest > paddy, indicating differences in their sources, deposition phases, and biogeochemical behavior in these soil systems. Although stable ^{127}I might not have fully equilibrated with Fukushima-derived ^{129}I, it likely still works as a proxy for the long-term fate of ^{129}I. Surficial soil ^{127}I content was well correlated to soil organic matter (SOM) content, regardless of land use type, suggesting that SOM might be an important factor affecting iodine biogeochemistry. Other soil chemical properties, such as Eh and pH, had strong correlations to soil ^{127}I content, but only within a given land use (e.g., within urban soils). Organic carbon (OC) concentrations and Eh were positively, and pH was negatively correlated to ^{127}I concentrations in surface water and rain samples. It is also noticeable that ^{127}I in the wet deposition was concentrated in both the deciduous and coniferous forest throughfall and stemfall water, respectively, comparing to the bulk rainwater. Further, both forest throughfall and stemflow water consisted exclusively of organo-iodine, suggesting all inorganic iodine in the original bulk deposition (~28.6% of total iodine) have been completely converted to organo-iodine. Fukushima-derived ^{239,240}Pu was detectable at a distance ~61 km away, NW of FDNPP. However, it is confined to the litter layer, even three years after the FDNPP accident-derived emissions. Plutonium-239,240 activities were significantly correlated with soil OC and nitrogen contents, indicating Pu may be associated with nitrogen-containing SOM, similar to what has been observed at other locations in the United States. Together, these finding suggest that natural organic matter (NOM) plays a key role in affecting the fate and transport of I and Pu and may warrant greater consideration for predicting long-term stewardship of contaminated areas and evaluating various remediation options in Japan.

* Corresponding author.
E-mail address: xuchen66@tamu.edu (C. Xu).

http://dx.doi.org/10.1016/j.jenvrad.2015.12.022
0265-931X/

1. Introduction

The catastrophic Tohoku earthquake of magnitude 9.0 hit off the east coast of Japan on March 11, 2011, triggering a tsunami that damaged the electrical network and the emergency diesel generators of the Fukushima Dai-ichi Nuclear Power Plant (FDNPP). Failure in cooling down reactor units caused numerous explosions, total damage of the FDNPP, and subsequent massive releases of radioactive substances into the atmosphere and to the Pacific Ocean. It was estimated that 153–160 PBq of ^{131}I, 5.71 GBq of ^{129}I, 13–15 PBq of ^{137}Cs (and ^{134}Cs), 1.0–2.4 TBq of ^{239,240}Pu, 1.1–2.6 TBq of ^{241}Pu, and 2.9–6.9 TBq of ^{238}Pu were emitted into the atmosphere, with less than 20% deposited over the landscape of Japan (Chino et al., 2011; Hou et al., 2013; Kato et al., 2012; Xu, S. et al., 2013; Zheng et al., 2013). This resulted in the Japanese Government classifying the FDNPP accident on the International Nuclear and Radiological Event Scale at the maximum level of 7, similar to the Chernobyl accident that occurred in 1986 in the Ukraine (Povinec et al., 2013).

Radioiodine ^{131}I and ^{129}I have half-lives of 8 d and 1.57×10^7 y, respectively, and they can enter the human body via food and drinking water and then selectively accumulate in the thyroid gland, resulting in a high radiation risk. Therefore, assessment of radioiodine behavior is of utmost importance to the dose reconstruction for people around the plant, especially for children. Speciation and concentration of iodine are essential to determine its mobility (Kaplan et al., 2010, 2014a; Schwehr et al., 2009; Shimamoto et al., 2011; Xu et al., 2011a, 2011b; Zhang et al., 2011; Zhang et al., 2013). Extensive iodine geochemistry studies have been conducted elsewhere in Japan, related to groundwater (Kozai et al., 2013), soil/sediment (Kodama et al., 2006; Shimamoto and Takahashi, 2008b; Takeda et al., 2015; Yamada et al., 1999; Yamaguchi et al., 2010), or in the soil/sediment-water system (Shimamoto and Takahashi, 2008a; Shimamoto et al., 2011; Takata et al., 2013; Takeda et al., 2015). Near the FDNPP area, iodine speciation studies have been conducted in seawater and atmospheric aerosols (Hou et al., 2013; Xu, S. et al., 2015); however, iodine speciation studies have not been conducted in the Fukushima Prefecture terrestrial environment. Also lacking, are detailed studies relating relevant soil properties in this region to iodine speciation.

As some mixed uranium (U) and plutonium (Pu) oxide (MOX) fuel was used in one of the reactors (Unit 3) that experienced hydrogen explosions, there was considerable public concern that one of the most hazardous elements, Pu, may have been released into the environment (Yamamoto et al., 2014, 2012). Within a few days after the reactor hydrogen explosions, Pu was transported in the atmosphere as far as 120 km distance by aerosol and wind (Shinonaga et al., 2014). Plutonium isotopes present a large risk for internal radiation exposure via ingestion of contaminated crops or by inhalation (Zheng et al., 2012). Yamamoto et al. (2012) detected trace amounts of Pu originating from the accident, mainly in surface soil samples (0–5 cm) collected in Iitate Village outside the 20-km exclusion zone, and in a few limited soil samples from Okuma Town, 2–5 km from the FDNPP. Zheng et al. (2012) reported the isotopic evidence for the release of Pu into the atmosphere and subsequent deposition on the ground 20–30 km northwest and south of the FDNPP. The Pu was mainly confined to the litter layer or soil surface. Interestingly, it was suggested that Pu content and isotope ratios differ considerably even for very close sampling locations, largely related to the soil vegetation (Schneider et al., 2013). As Fukushima-derived ^{234,240}Pu was strongly diluted and the isotopic signatures were altered by the pre-Fukushima global fallout, it is difficult yet very important to resolve factors that control the long-term migration of Pu in the Fukushima Prefecture.

Cesium-134 and cesium-137, with half-lives of 2.06 and 30.1 y, respectively, have caused the largest public concerns, because they constitute the majority of the external and internal radiation doses from the FDNPP accident. It is expected that they will have a deleterious effect on agriculture and livestock farming, and thus, human life, for decades to come (Kitamura et al., 2014; Yasunari et al., 2011). Numerous field measurement and modelling studies have quantified depth distributions and vertical migration of Fukushima-derived radiocesium (Kato et al., 2012; Kitamura et al., 2014; Matsuda et al., 2015; Niimura et al., 2015). However, different land uses significantly affect the distribution and migration of radioisotopes (Kitamura et al., 2014), yet has not been studied at the Fukushima Prefecture. Moreover, Schneider et al. (2013) suggested that Pu releases and fallout from the FDNPP were very different from those of Cs, which is in contrast to co-existing patterns of Cs and Pu in the environment of the Savannah River Site (SRS) in South Carolina, U.S (Savannah River Nuclear Solutions, 2013). They contend that Pu was released in a single event, primarily in the form of particulate Pu, which lead to non-uniform Pu contamination. This was very different from the volatile radionuclides, radiocesium and radioiodine, which were released from the pressure vessels over several days in the course of the early venting operations. Even where there is Pu released, its associated particle size is also very different from that of Cs-associated particles (Niimura et al., 2015; Shinonaga et al., 2014; Xu, S. et al., 2015; Zheng et al., 2013).

The Japanese Government still plans to include nuclear power as a core energy source and expects that it will provide up to 22% of the country's electricity supply by 2030. In addition, the country faces the enormous challenge of remediating residual radioactivity at the FDNPP site and devising and implementing sounder defensive plans for those reactors that are located in earthquake faults and volcano regions. It is thus necessary to understand the factors that affect iodine and plutonium speciation and effectively predict their long-term transport and fate in the environment. For this purpose, four types of soils were selected within a 75- km radius (urban, paddy, deciduous forest, and coniferous forest), northwest of the FDNPP (Fig. 1), and analyzed for stable iodine concentrations, speciation and total ^{239,240}Pu activity concentration and isotopic ratios (^{240}Pu/^{239}Pu). River water (from forest sub-catchment) and rainwater samples were also collected and analyzed for iodine concentrations and speciation. Iodine-129 was not measured due to limitation of our instrumental technique. However, by studying the biogeochemical characteristics and controls of ^{127}I, one can predict the fate and behavior of sporadic post-accident ^{129}I in the long term (Hou et al., 2001; Hu et al., 2007, 2005; Kaplan et al., 2011; Kaplan et al., 2014b; Zhang et al., 2014; Zhang et al., 2013). A number of ancillary chemical parameters were measured, including pH, oxidation-reduction potential, dissolved organic carbon (DOC). The objective is to provide insight into the soil and aqueous geochemical conditions acting on iodine and Pu that could influence their distribution and mobility in the environment. Cesium-134 and cesium-137 activities in these samples were also determined, and their biogeochemical behavior was then compared with that of iodine and Pu.

2. Materials and methods

2.1. Study sites, field sampling and chemical properties analysis

Our study sites are located in eastern part of Fukushima City and Oguni forest, in the northwestern region of the Fukushima Prefecture (Fig. 1). They are located between 53 and 63 km from the FDNPP within a 75- km radius area. Seven surface soil samples (<4 cm) were randomly collected from the urban area of Fukushima

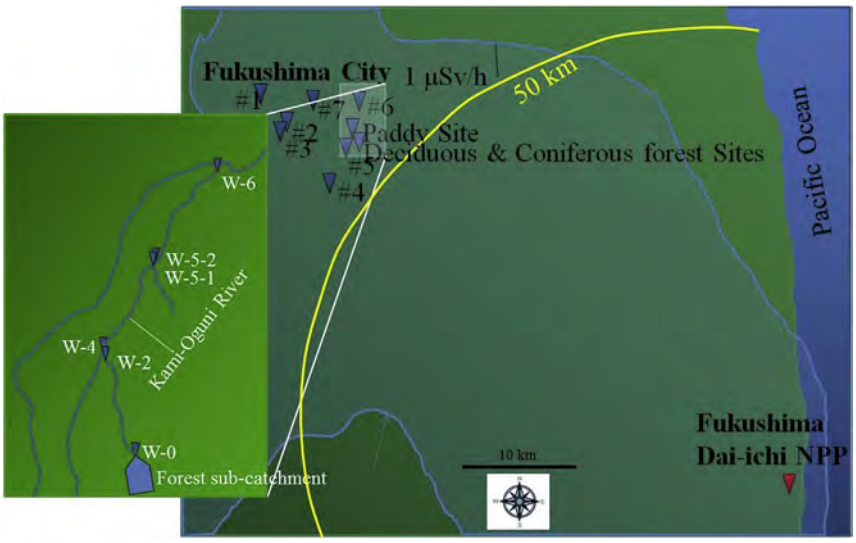

Fig. 1. Location of the study site. (#1 to #7 are urban soil sampling sites; W-0, W-2, W-4, W-5-1, W-5-2, and W-6 are river water sampling sites of Oguni River; the irregular blue lines represent the radiation dose rate contour at 1 μSv/h of the Fukushima Dai-ichi NPP accident at 1 μSv/h) (For interpretation of the references to colour in this figure legend, the reader is referred to the web version of this article).

City, including a sidewalk west of Fukushima station, a residential area, an industrial area, two roadside locations, and two public parks, on March 20, 2012. Soil profiles from a paddy field, a deciduous forest (*Quercus serrata*, *Zelkova serrata*, *Carpinus tschonoskii*, *Acer pictum*), and a coniferous forest (*Cryptomeria japonica*) were collected using a DIK-110C liner sampler (Daiki Rika Kogyo Co., Ltd., Japan) with a PVC sample tube, on March 13, 2013. These sites are located 4–5 km southeast of the center of Fukushima City. The coniferous site is only ~24 m southwest of the deciduous site. Both sites are in the same valley, with the deciduous site on a southeast facing slope and the coniferous site on a southwest facing slope. During the period of the FDNPP accident (March 2011) and the sampling dates (March 2012 and March 2013), there were no many leaves on the deciduous trees to scavenge atmospheric deposition. Conversely, the conifers have leaves year round. During March, rice paddies do not have standing water. Instead, there is only plant stubble in open dry fields. In order to provide sufficient samples (~10 g for each) for $^{240}Pu/^{239}Pu$ isotopic ratio determination, extra samples were collected the following year (March, 2014), at the deciduous forest and coniferous forest sites.

Surface water was sampled at different points along the flow path from a tributary of the Oguni River, on March 21, 2014. Additionally, three types of rainfall samples were collected: bulk deposition, stemflow, and throughfall. The bulk deposition sample was collected from an open space area, the stemflow was water that trickled down the stem and the throughfall was water that first came in contact with the tree canopy. These samples were collected from multiple randomly-selected trees in the deciduous and coniferous forests, respectively. More specifically, throughfall samples were collected using a funnel-shaped throughfall trap with a 0.2-m diameter opening. Stemflow samples were collected with a stemflow-trap made by attaching a 22.5-mm diameter by 1.5-m long plastic tubing around the circumference of the tree at breast height. Stemflow water entered the plastic tubing through a series of small holes, and then was directed through a second tubing into a collection bottle. Upon collection all water samples were filtered immediately through a 0.7-μm pre-combustered GF/F glass fiber filters (Whatman, Littlechalfont, UK) and kept frozen. The maximum amount of water sample collected in each sample was 4 L(Endo et al., 2015). All soil and water samples were stored on ice and shipped overnight to Texas A&M University at Galveston (TAMUG) for analysis. Routine environmental water analyses were conducted using standard methods; pH and oxidation-reduction potential (ORP) were measured using an OAKTON 510 pH/mV/°C meter and DOC with a Shimadzu TOC-L analyzer.

Soil samples were oven-dried at 60 °C, homogenized and the < 2-mm sieved fraction was used for subsequent analysis. Both ORP and pH were measured on 1:1 solid: water (18.2 MΩ) slurries. Total carbon and nitrogen contents were measured using a Perkin Elmer CHNS/O 2400 analyzer and organic carbon (OC) content was determined after a direct acidification step (Ryba and Burgess, 2002). Inorganic carbon was then calculated as the difference between total carbon and organic carbon contents.

Gamma-ray emissions of ^{134}Cs and ^{137}Cs at energies of 604 keV and 662 keV, respectively, were determined by a high purity germanium coaxial gamma ray detector (GCW3024, Canberra Eurisys, Meriden, U.S.A.), coupled to a multichannel analyzer (DSA 1000, Canberra Eurisys, Meriden, U.S.A.). The measurement system was calibrated with standard ^{134}Cs (Cat. #: 7134) and ^{137}Cs (Cat. #: 7137) sources purchased from Eckert & Ziegler Isotope Products Inc. (CA, U.S.A.). Both ^{134}Cs and ^{137}Cs activities were decay-corrected to March 11, 2011.

2.2. Determination of iodine speciation

Determination of aqueous I^- and IO_3^- followed the procedure in Zhang et al. (2010). This method has a detection limit of 0.04 μg/L $^{127}I^-$ and 0.14 μg/L $^{127}IO_3^-$. Aliquots of each sample were analyzed to determine I^-, total inorganic iodine (I^- and IO_3^-), and total iodine (I^-, IO_3^-, and organo-I), respectively. For the I^- analysis, I^- was oxidized by 2-iodosobenzoate to I_2, and then N,N-dimethylaniline was added to bind the I_2 to form 4-iodo-dimethylaniline. The resulting derivative was extracted with cyclohexane and measured using a Finnigan Trace GC coupled with Polaris Q EI-MS from Thermo Scientific. Using a second subsample, total inorganic iodine was measured by reducing IO_3^- to I^- by the addition of sodium meta-bisulfite. The solution I^- was measured using the same derivatization method described above. Concentration of IO_3^- was calculated as the concentration difference between the total inorganic iodine and I^-. In the third subsample, total iodine

concentrations were determined directly using an inductively coupled plasma mass spectrometer (ICP-MS) Thermo X series II, equipped with an Xt cone and SC4 DX autosampler with PC^3 spray chamber kit. Organo-I concentration was calculated based on the concentration difference between the total iodine and the total inorganic iodine. The detection limit of this method was determined as 0.35 μg/L organo-^{127}I.

Total iodine (TI) content in the soil was measured by catalytically combusting and converting all the iodine in the soil into inorganic iodine species (Zhang et al., 2010), the total concentrations of which were then detected by the GC–MS derivatization method or ICP–MS method described above. Measurement accuracy was certified by determination of total iodine in a NIST Standard Reference Material (SRM® 2709) San Joaquin Soil (TI reported as 5 μg/g), and the difference between the experimental and reported values was well within 3%.

2.3. Determination of total ^{239,240}Pu and ^{240}Pu/^{239}Pu isotopic ratios

A 0.5-g (for α spectrometry) or 10-g (for ICP-MS) soil or litter sample was ashed in a ceramic crucible at 600 °C for >16 h. Then ^{242}Pu was added as a yield tracer to the sample and the sample was acid-digested according to Xu, C. et al. (2015). Plutonium isotopes were separated from other radionuclides (e.g., ^{238}U and ^{241}Am) with UTEVA column (Cat. #: UT-C50-A, Eichrom, USA) (Lee et al., 2011; Morgenstern et al., 2002). The column eluent was then used in conducting α spectrometry for total ^{239,240}Pu activity analyses, and ICP-MS for ^{240}Pu and ^{239}Pu analyses (Xu, C. et al., 2015).

Because ^{239}Pu and ^{240}Pu cannot be resolved by α spectrometry, their activity was reported as combined ^{239,240}Pu activity. The activity of the blank, which was run throughout the whole procedure, was subtracted from each experimental sample. Plutonium-239,240 activity was calculated based on the known activity of ^{242}Pu added as the yield tracer and the peak area ratio of ^{239,240}Pu over ^{242}Pu. The detection limits for ^{239,240}Pu and ^{242}Pu, as determined by analyzing seven samples with known concentrations approximating the expected limit of detection and calculating the product of t value (3.14 for a 99% confidence interval) and the standard deviation, are 1.2×10^{-4} Bq/g and 5.0×10^{-4} Bq/g, respectively.

Isotopic ratios of ^{240}Pu/^{239}Pu of selected samples were measured using an ICP-MS (Xseries II, Thermo Scientific, USA) equipped with a PC^3 sample inlet system. For this purpose, Pu eluent after column separation was evaporated to incipient dryness and re-constituted with 2 mL 2% HNO_3. The detection limits for ^{239}Pu, ^{240}Pu and ^{242}Pu, as determined by analyzing seven samples with known concentrations approximating the expected limit of detection and calculating the product of t value (3.14 for a 99% confidence interval) and the standard deviation, are 0.0025, 0.0015, 0.0016 pg/g, respectively.

3. Results and discussion

3.1. Environmental factors affecting iodine concentrations and speciation in soil

Iodine distributions throughout the paddy and deciduous forest soil profiles were fairly uniform, whereas the coniferous forest soil profile showed a marked increase below 10 cm (Fig. 2a). Two of the main sources of terrestrial ^{127}I are mineral dissolution and deposition of seawater aerosols transported in the atmosphere (ATSDR, 2004). Because these locations are inland, the ^{127}I depth profile of diminishing concentrations with depth, characteristic of seawater aerosol deposition as the main ^{127}I source, was not observed. The ^{127}I concentration profile from the coniferous forest suggests that a subsurface strata may be elevated in ^{127}I. The pH of paddy and deciduous forest soils increased with depth to 15–20 cm below the surface, whereas the pH of the coniferous forest soil displayed a subsurface maximum layer at ~7.5 cm (Fig. 2b). Eh values of deciduous forest soils decreased with depth, while those of coniferous forest soil decreased first and then increased (Fig. 2c). Eh values of paddy soil showed a similar decreasing trend in the upward 11 cm as those of deciduous forest soil, yet lack of data below 15 cm makes it hard to determine the downward trend. It is common to see an inverse relationship between soil iodine and pH due to lower pH levels increasing the anion exchange capacity of many pH-dependent charge soils, such as common in much of Japan (Wada, 1985), and a desorption of soil iodine into solution when soil Eh falls below around 150 mV (Ashworth, 2009). However, neither pH nor Eh values were simply related to iodine concentrations in the soil depth profiles examined here, suggesting that complex, interactive factors or unknown processes control iodine concentrations vertically in these soils. In addition, different land uses and anthropogenic disturbances will also affect the iodine depth distribution. For example, the plowing activity in the paddy soil leads to a homogeneous depth profile for OC and I, yet Eh and pH values did show significant concentration trends with depth (Fig. 2b and c), suggesting both properties form vertical gradients within the soil column following plowing more quickly than OC and I. Noticeably, from the horizontal perspective, iodine concentrations of the seven urban surface soil samples (<4 cm) were negatively correlated with pH values ($p = 0.01$) (Fig. 2d), and significantly positively correlated with Eh values ($p = 0.0055$) (Fig. 2e).

Content of OC (%, wt) decreased in the coniferous forest soil from 12.5% to 1.77% over the depth profile of 1.5 cm–16 cm below the surface (Fig. 2f). In contrast, there was a less dramatic decrease in OC concentration with depth in the deciduous forest, and OC concentrations did not change significantly with depth in the paddy soil (Fig. 2f). In addition, the depth profile of iodine did not correlate with that of OC contents (Fig. 2f vs. 2a). This is in contrast to what was found in wetland soils (Kaplan et al., 2014b) and a Japanese hot spring soil (Shimamoto et al., 2011), in which iodine concentrations correlate well with those of OC in individual soil profiles. However, it could have been due to limited sample size within each type of land use (i.e., only one soil profile was collected for each land use). Nevertheless, if one takes the values of all surface soils (<4 cm, urban, paddy, deciduous and coniferous), iodine concentrations were correlated with OC contents ($R = 0.61$, $p < 0.05$) (Fig. 2g). Therefore, it is likely that soil organic matter (SOM) is the universally dominant environmental factor in affecting iodine retention by soil in this area, whereas the effects of pH or Eh are more restricted in soils of the same type or land use (e.g., urban soil).

Comparing the surface (<4 cm) total soil iodine concentrations (Table 1), the four types of soil ranked in the order of coniferous (10.4 μg/g) > deciduous (4.89 μg/g) > urban soil (2.06 ± 0.70 μg/g) > paddy soil (1.74 μg/g). Noticeably, total iodine concentrations in each individual depth section of the coniferous forest soil column were 1.3–5.3 times higher, respectively, than those of the deciduous forest soil column (Table 1). This seems to be partially explained by an elevated OC content (1.5–3.3 times) in the coniferous forest soil with respect to the deciduous forest soil. However, the I:C ratios, which ranged from 9.4 to 124×10^{-6}, with a mean value of 49×10^{-6} for deciduous forest soils and from 7.9 to 142×10^{-6} with a mean value of 58.4×10^{-6} for coniferous forest soils, were not constant throughout the soil column (Fig. 2h). It is thus possible that total I levels in different types of forest soil may not only depend on OC content but also on the SOM composition and the degree to which SOM can be iodinated. Indeed, Montelius et al. (2015) reported that coniferous forest soil scavenges another halogen from atmospheric depositions, chlorine, to a greater extent

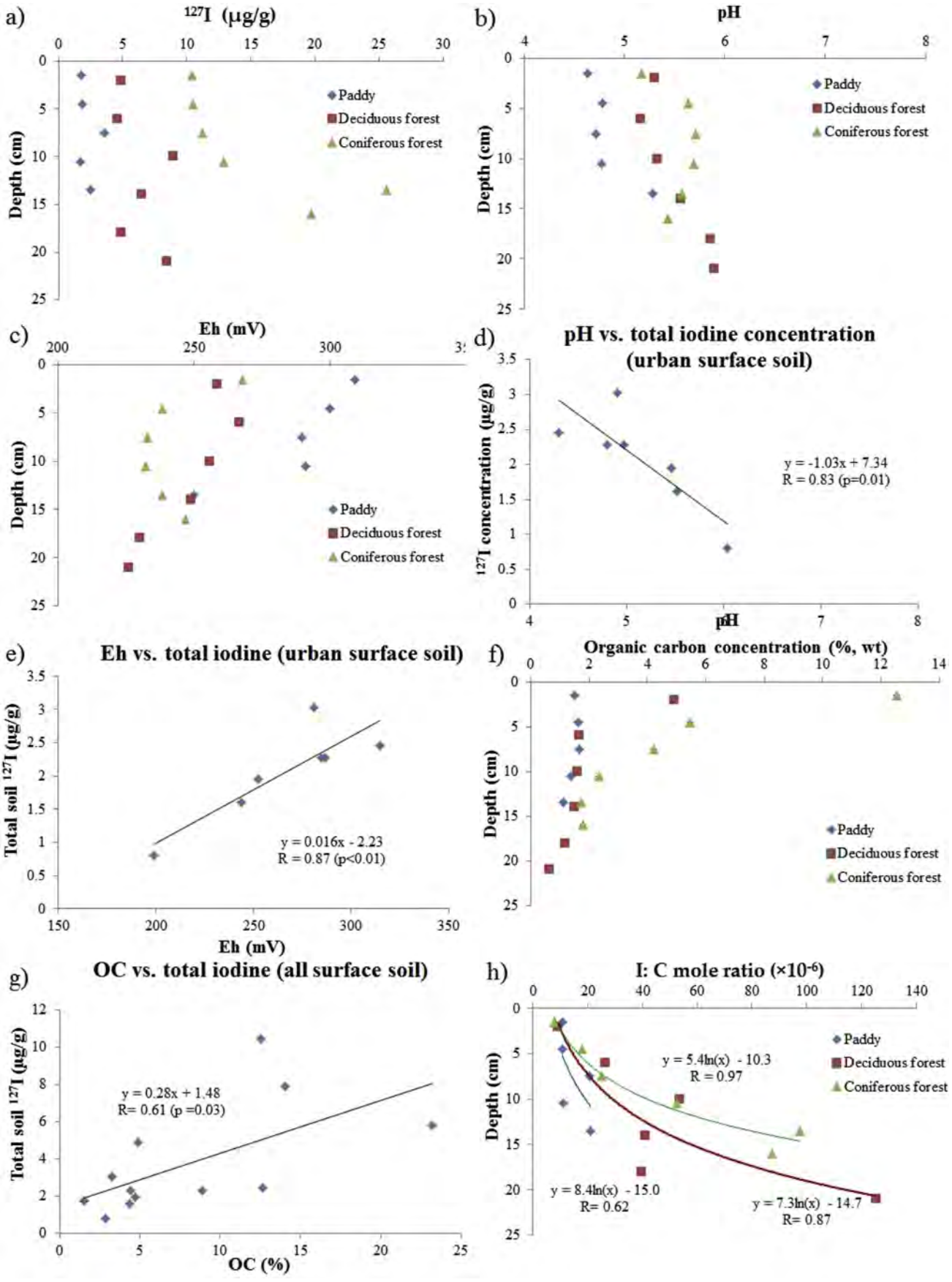
a)
^{127}I (μg/g)
Depth (cm)
Paddy
Deciduous forest
Coniferous forest
b)
pH
Depth (cm)
Paddy
Deciduous forest
Coniferous forest
c)
Eh (mV)
Depth (cm)
Paddy
Deciduous forest
Coniferous forest
d)
pH vs. total iodine concentration (urban surface soil)
^{127}I concentration (μg/g)
pH
y = -1.03x + 7.34
R = 0.83 (p=0.01)
e)
Eh vs. total iodine (urban surface soil)
Total soil ^{127}I (μg/g)
Eh (mV)
y = 0.016x - 2.23
R = 0.87 (p<0.01)
f)
Organic carbon concentration (%, wt)
Depth (cm)
Paddy
Deciduous forest
Coniferous forest
g)
OC vs. total iodine (all surface soil)
Total soil ^{127}I (μg/g)
OC (%)
y = 0.28x + 1.48
R= 0.61 (p =0.03)
h)
I: C mole ratio (×10^{-6})
Depth (cm)
Paddy
Deciduous forest
Coniferous forest
y = 5.4ln(x) - 10.3
R = 0.97
y = 8.4ln(x) - 15.0
R= 0.62
y = 7.3ln(x) - 14.7
R= 0.87

than deciduous forest soil. Actually, mole ratios of I: C exponentially increase with depth in both forest soil profiles (Fig. 2h). Similar trends were also found by Shetaya et al. (2012). Soil organic matter at deeper depths are commonly more refractory to turnover and thus could have more time to fix iodine. Alternatively, this refractory form of SOM could be more efficient at iodine scavenging. Thus, although SOM is likely the primary environmental factor of iodine geochemical behavior, bulk SOM measurements do not adequately describe the soil iodine fixation capacity of these Japanese soils. Specific functional groups of SOM were previously found to be directly or indirectly involved in iodine transformation and binding (conversion of I^- or IO_3^- to organo-iodine) (Xu, C. et al., 2013; Xu et al., 2012). Thus, characterization of SOM components that are responsible for iodine transformation and binding in these Japanese soil samples is warranted.

By investigating 20 Chinese soils covering a wide variety of soil types, Dai et al. (2009) discovered that SOM had a significant positive effect on I^- sorption, but a negative effect on IO_3^- sorption. In contrast, others have found that SOM is the determinant factor that positively influences iodine retention in soil, regardless of the initial iodine speciation (I^- or IO_3^-) (Schwehr et al., 2009; Xu, C. et al., 2013; Xu et al., 2011a, 2011b, 2012; Yamaguchi et al., 2010; Zhang et al., 2011). The discrepancy might result from different experimental durations of the various studies. According to Shetaya et al. (2012), IO_3^- uptake by soil was initially preceded by an instantaneous sorption reaction, which is positively controlled by Fe/Mn oxide content, but negatively related to pH and SOM content. Then it was followed by a slow time-dependent process which was positively controlled by SOM contents. Uptake of I^- by soil followed a fast overall reaction suggesting the two processes might not be distinctly separated. The slow process can occur over hours to days, while the fast one over minutes to hours. As a matter of fact, by investigating nine various soil samples, Shetaya et al. (2012) observed that given enough reaction time, both I^- and IO_3^- were ultimately incorporated into SOM. Therefore iodine uptake by soil is speciation-driven, as well as contact time-dependent. Wet deposition is one of the main sources of iodine to the surface soil (Shetaya et al., 2012). Rainfall infiltrating the soil and draining out of it can range from hours to days, depending on soil texture and SOM contents. Besides soil properties, iodine speciation in the rainfall is another vital factor that affects retention of iodine in the surface soil.

3.2. Factors affecting iodine concentration and speciation in rainwater and surface water

A representative wet deposition event collected during the same season that the other samples were collected had organo-iodine as the dominant species (71.5% of total iodine), followed by I^- (20.9%) and IO_3^- (7.62%) (Table 2). This agrees with the findings of Gilfedder et al. (2007) that the majority of iodine in rain and snow collected worldwide was associated with organic matter (average 56%) followed by I^- (average 27%). However, there are other studies in which IO_3^- was shown to be the dominant species in the bulk precipitation. It is likely due to the facts that their samples were collected over the sea (Baker et al., 2001; Campos et al., 1996) or in areas in very close vicinity of the ocean (Hou et al., 2009; Truesdale and Jones, 1996), whereas our sampling sites are relatively more inland (>75 km away from the shore), thus less affected by marine atmosphere. Nevertheless, once the precipitation entered the soil, I^- was more quickly converted into organo-iodine than IO_3^- (Shetaya et al., 2012). Throughfall and stemflow of both forests exclusively contained organo-iodine (Table 2). Organo-iodine compounds, of both "autochthonous" (derived from the interaction of I^-, IO_3^- and SOM) and "allochthonous" (derived from direct deposition) sources, were then more retained than inorganic iodine species (Hu et al., 2005; Zhang et al., 2011), during drainage or surface run-off events.

This study, for the first time, provides iodine speciation data on the throughfall and stemflow of both deciduous and coniferous plantation. There was a slight increase in iodine concentration in the deciduous throughfall (2.65 μg/L) and almost a three-fold increase in coniferous throughfall (6.41 μg/L), compared to the bulk deposition (2.28 μg/L). Iodine being less concentrated in deciduous throughfall than in coniferous throughfall is due to the winter samplings (March, 2014) occurring when the deciduous forest canopy was thin (section 2.1), while the coniferous canopy was still frondent. This is supported by ^{137}Cs data (Table 2), as FDNPP-derived ^{137}Cs was more captured in the coniferous canopy, thus showing a much lower ^{137}Cs activity concentration (283 Bq/L) in the coniferous throughfall, whereas ^{137}Cs concentration in deciduous throughfall (1.24×10^3 Bq/L) is close to that in the bulk deposition (1.69×10^3 Bq/L). Iodine concentrations increased by a factor of 5.1 and 2.8 in the stemflow of deciduous (11.7 μg/L) and coniferous (6.34 μg/L) trees, respectively, compared to that in the bulk deposition. The observation that iodine concentrations in throughfall and stemflow of both types of forests are generally higher than those in the bulk deposition, partly contributed to the evaporative concentration process by these plants (through loss of water in the rainfall), and their scavenging fine mists which are enriched in iodine yet might not be collected by the open rainfall collector (Neal et al., 1990). Most importantly, inorganic iodine, present in the bulk deposition (28.6% of total iodine) was completely converted to organo-iodine after the rainwater contacted the leaves or stems of the trees, indicative of fast transforming iodine speciation by organic matter present in the throughfall and stemflow solution. Concomitantly, their OC contents dramatically increased compared to that of bulk deposition, by a factor of 1.4 and 10.4 for deciduous throughfall and stemflow, and a factor of 7.0 and 6.6 for coniferous throughfall and stemflow, respectively (Table 2). Such increases in dissolved organic carbon (DOC) concentrations of forest throughfall and stemflow relatively to the bulk deposition were previously reported (Bergkvist and Folkeson, 1992; Ciglasch et al., 2004; Guo et al., 2005; Michalzik et al., 2001; Qualls et al., 1991), possibly caused by dissolution of soluble organic material deposited on the surface of the plants, soluble animal or microbially-derived organic material in the canopy, or leaching of leaves, needles or stems. Not only did the quantity of rainwater DOC change after it intercepted with the canopy, but the chemical properties and compositions of the organic matter were also altered, driven by various abiotic and biotic processes. For example, the aromaticity and humification indices of both deciduous and coniferous throughfall and stemflow increased significantly compared to the bulk deposition, suggesting that organic matter in the forest throughfall and stemflow solutions contains more aromatics and refractory condensed aromatics (Bischoff et al., 2015; Lv et al., 2014). Aromatics likely then scavenged iodine through electrophilic substitution via abiotic and

Fig. 2. a) Depth profile of ^{127}I concentration (μg/g), b) depth profile of pH, c) depth profile of Eh of paddy soil, deciduous forest soil and coniferous forest soil, d) correlation between pH values and total soil ^{127}I (μg/g) of seven urban surface soil (<4 cm), e) correlation between Eh and total soil ^{127}I (μg/g) of seven urban surface soil (<4 cm), f) depth profile of organic carbon (OC, % wt) contents of paddy soil, deciduous forest soil and coniferous forest soil, g) correlation between OC (%, wt) and total soil ^{127}I (μg/g) for all surface soil (seven urban soil, one paddy soil, one deciduous forest soil, and one coniferous forest soil, h) depth profile of I:C mole ratio.

Table 1
Soil chemical information.

Sampling date (day/month/year)	Land Category	Site Code	Depth (cm)	^{127}I (μg/g)	^{239,240}Pu (Bq/kg)	^{240}Pu/^{239}Pu	Organic carbon (%, wt)	Inorganic carbon (%, wt)	Nitrogen (%, wt)	pH	Eh (mV)	^{137}Cs (Bq/kg)	^{134}Cs (Bq/kg)	^{134}Cs/^{137}Cs
3/20/2012	Urban	#1	<4 cm	0.81	0.22 ± 0.01	n.a.	2.89 ± 0.61	0.71 ± 0.01	0.09 ± 0.02	6.03	199	1.36×10^5	1.34×10^5	0.99
	Urban	#2	<4 cm	3.03	0.21 ± 0.03	n.a.	3.25 ± 0.02	n.d.	0.27 ± 0.02	4.90	281	2.59×10^4	2.70×10^4	1.04
	Urban	#3	<4 cm	2.28	0.06 ± 0.00	n.a.	4.40 ± 0.51	0.49 ± 0.04	0.43 ± 0.01	4.97	287	4.18×10^4	4.81×10^4	1.15
	Urban	#4	<4 cm	2.46	n.d.	n.a.	12.6 ± 2.6	0.42 ± 0.01	0.81 ± 0.30	4.30	315	2.74×10^5	2.68×10^5	0.98
	Urban	#5	<4 cm	2.28	0.03 ± 0.00	n.a.	8.88 ± 1.58	n.d.	0.53 ± 0.08	4.80	285	3.46×10^5	3.28×10^5	0.95
	Urban	#6	<4 cm	1.95	0.1 ± 0.01	n.a.	4.69 ± 0.22	n.d.	0.29 ± 0.01	5.46	252	6.97×10^4	6.97×10^4	1.00
	Urban	#7	<4 cm	1.61	0.12 ± 0.01	n.a.	4.36 ± 1.59	n.d.	0.26 ± 0.01	5.52	244	4.52×10^4	1.36×10^5	0.99
3/13/2013	Paddy		0–3	1.74	0.19 ± 0.05	n.a.	1.50 ± 0.30	0.33 ± 0.01	0.17 ± 0.01	4.63	309	3.51×10^3	3.34×10^3	0.95
			3–6	1.87	0.13 ± 0.04	n.a.	1.63 ± 0.18	n.d.	0.13 ± 0.02	4.78	300	2.84×10^3	2.59×10^3	0.91
			6–9	3.59	0.17 ± 0.05	n.a.	1.64 ± 0.29	n.d.	0.14 ± 0.01	4.72	290	3.14×10^3	2.96×10^3	0.94
			9–12	1.67	0.19 ± 0.06	n.a.	1.38 ± 0.02	0.19 ± 0.05	0.14 ± 0.01	4.77	291	2.38×10^3	2.17×10^3	0.91
			12–15	2.48	0.11 ± 0.01	n.a.	1.10 ± 0.08	0.08 ± 0.01	0.10 ± 0.00	5.28	250	125	108	0.86
	Deciduous forest		litter	4.84	1.31 ± 0.25	0.34 ± 0.02	n.a.	n.a.	n.a.	n.a.	n.a.	2.32×10^4	2.21×10^4	0.95
			0–4	4.89	1.11 ± 0.01	0.18 ± 0.01	4.90 ± 0.41	0.08 ± 0.02	0.31 ± 0.01	5.30	259	7.21×10^3	8.26×10^3	1.15
			4–8	4.61	0.61 ± 0.29	n.a.	1.64 ± 0.50	0.34 ± 0.01	0.15 ± 0.03	5.16	267	630	619	0.98
			8–12	8.94	0.69 ± 0.00	n.a.	1.58 ± 0.05	0.12 ± 0.02	0.13 ± 0.00	5.33	256	426	441	1.04
			12–16	6.46	0.24 ± 0.06	n.a.	1.48 ± 0.17	0.11 ± 0.01	0.14 ± 0.01	5.56	249	238	206	0.87
			16–20	4.88	0.22 ± 0.10	n.a.	1.16 ± 006	n.d.	0.09 ± 0.02	5.86	230	62	45	0.72
			20–22	8.42	0.11 ± 0.04	n.a.	0.64 ± 0.06	n.d.	0.05 ± 0.01	5.90	226	14	11	0.76
	Coniferous forest		litter	n.a.	0.19 ± 0.09	n.a.	n.a.	n.a.	n.a.	n.a.	n.a.	7.37×10^4	678×10^4	0.92
			0–3	10.4	1.01 ± 0.00	0.16 ± 0.06	12.53 ± 0.93	2.17 ± 0.04	0.73 ± 0.04	5.17	268	8.91×10^3	8.63×10^3	0.97
			3–6	10.5	1.26 ± 0.15	0.16 ± 0.06	5.44 ± 1.31	1.85 ± 0.33	0.44 ± 0.03	5.64	238	835	871	1.04
			6–9	11.2	0.66 ± 0.05	n.a.	4.22 ± 0.47	n.d.	0.28 ± 0.00	5.71	233	198	156	0.79
			9–12	12.9	0.19 ± 0.04	n.a.	2.32 ± 0.56	1.39 ± 0.34	0.27 ± 0.04	5.69	232	85	82	0.96
			12–15	25.6	0.02 ± 0.03	n.a.	1.71 ± 0.31	0.40 ± 0.04	0.19 ± 0.01	5.57	238	37	27	0.72
			15–17				1.77 ± 0.07	0.11 ± 0.07	0.19 ± 0.01	5.43	247	19	18	0.93

n.d., not detectable; n.a., not available (sample amount not enough for analysis). Error for ^{137}Cs and ^{134}Cs is within 3% and for ^{127}I is <10%.^{137}Cs and ^{134}Cs are decay-corrected to March 11, 2011. For ^{240}Pu/^{239}Pu determination, samples were collected on March 21, 2014, at the same locations of the two forests.

Table 2
Chemical properties and iodine speciation of wet deposition and Oguni River water.

Sample	DOC (mg/L)	pH	Eh (mV)	^{137}Cs (Bq/L)	Iodine concentration (μg/L)				Ratio to total iodine (%)		
					Total	I^-	IO_3^-	Organo-iodine	I^-	IO_3^-	Organo-iodine
Wet deposition											
Bulk deposition	6.18	5.34	567	1.69×10^3	2.28	0.48	0.17	1.63	20.9	7.62	71.5
Throughfall of deciduous forest	8.54	5.34	549	1.24×10^3	2.65	n.d.	n.d.	2.65	0.00	0.00	100
Throughfall of coniferous forest	43.4	5.30	550	283	6.41	n.d.	n.d.	6.41	0.00	0.00	100
Stemflow of deciduous forest	64.5	3.18	693	179	11.7	n.d.	n.d.	11.7	0.00	0.00	100
Stemflow of coniferous forest	41.0	5.06	562	123	6.34	n.d.	n.d.	6.34	0.00	0.00	100
Oguni River water											
W-0 (head water)	1.14	7.02	576	8.12×10^3	0.53	0.16	0.03	0.34	31.0	5.02	64.0
W-2 (upstream)	1.19	6.25	618	828	0.90	0.19	0.17	0.54	20.8	19.2	60.0
W-4 (upstream)	1.28	6.25	613	443	1.03	0.11	0.35	0.57	10.9	33.8	55.3
W-5-1 (before joining a tributary)	1.53	6.28	619	105	0.67	0.06	0.30	0.32	8.60	44.1	47.3
W-5-2 (after joining a tributary)	1.53	6.26	618	7	0.71	0.04	0.00	0.71	6.02	0.00	94.0
W-6 (downstream)	1.47	6.26	621	3	1.50	0.20	0.41	0.89	13.5	27.3	59.2
Average (river water only)	1.36 ± 0.17	6.39 ± 0.31	611 ± 17	(1.58 ± 3.22) × 10^3	0.89 ± 0.35	0.13 ± 0.07	0.21 ± 0.17	0.56 ± 0.22	15.1 ± 9.26	21.6 ± 16.9	63.3 ± 16.1

enzymatic pathways (Xu, C. et al., 2013; Xu et al., 2011b; Xu et al., 2012). Therefore, the presence of high NOM on the plant surfaces and their unique chemical properties (e.g., aromatics) might be another reason to explain the elevated ^{127}I concentrations in the forest throughfall and stemflow. Additional long-term iodine speciation analysis of the rainfall and obtaining detailed information on the related plant organic matter in the forest throughfall and stemflow will be needed in future work.

Dissolved organic carbon (DOC) concentrations (1.14–1.53 mg/L) in the Oguni River water, which receives discharge from the adjacent forest sub-catchment (Fig. 1), was lower than the average DOC concentration of typical world rivers (4.2–5.75 mg/L) (Meybeck, 1982, 1988). The downstream tributary had slightly higher DOC concentrations (W-5-1, W-5-2 and W-6) than the upstream (W-0, W-2, and W-4) (Table 2). Total ^{127}I ranged from 0.53 to 1.5 μg/L, comprised mostly of organo-iodine (63.3 ± 16.1% of total I). Both DOC and total iodine concentrations measured in the river and tributaries was much lower than that in the bulk deposition, throughfall and stemflow, suggesting a possible dilution by the discharge from the forest sub-catchment, in which organic matter

and iodine might have been scavenged by the forest soil. Total iodine concentrations of the six surface water and five wet deposition samples shown in Table 2 were positively correlated with Eh and OC values ($p = 0.0001$), whereas they are negatively correlated with pH values (Fig. 3). These results indicate that pH, Eh and OC cooperatively affect the geochemical behavior of iodine in surface water and wet deposition.

Cesium-137 activities in these samples were monitored to provide a comparison with the ^{127}I measurements (Table 2). The ^{137}Cs originated primarily from the FDNPP accident, whereas the ^{127}I had natural origins. The ^{137}Cs activity concentration decreased by about 27% and 83%, for deciduous and coniferous throughfall, and by about 89% and 92%, for deciduous and coniferous stemflow, respectively, compared to that of the bulk deposition. The consistently decreasing trend of ^{137}Cs activity concentration along the rainwater passage (i.e., bulk deposition > throughfall > stemflow) is in contrast to the behavior of the ^{127}I, where concentrations increased with precipitation passage through the canopy and along the plant stems. Moreover, the headwater (W-0) of Oguni River contains the highest ^{137}Cs activity concentration and it consistently decreased along the flowpath, suggesting a "point source" in the upstream region (Table 2). It is noteworthy to point out that stable iodine has not necessarily reached equilibrium with FDNPP-derived radioiodine (^{129}I). Our observation that there is a significant difference in the distribution of ^{137}Cs and ^{127}I does not necessarily reflect the same situation for ^{129}I and ^{137}Cs, both originating from FDNPP accident. However, the fact that ^{137}Cs activity concentration has shown no correlation to DOC concentrations supports that the two elements, Cs and I, apparently have very different biogeochemical behavior in these two forest ecosystems, and NOM seems to exert less important effects on the behavior of Cs than on iodine.

3.3. *Factors affecting plutonium scavenging by soil*

Plutonium-239,240 activity concentration in the four types of surface soil (<4 cm) ranked in the order of deciduous forest (>(1.11 ± 0.01) Bq/kg)> coniferous forest ((1.01 ± 0.00) Bq/kg) > paddy ((0.19 ± 0.05) Bq/kg) > urban (0.12 ± 0.08) Bq/kg) (Table 1). This is quite different from the distribution of ^{134}Cs and ^{137}Cs in the surface soils (0–3 cm): urban surface soil contains the highest activity concentration of both Cs isotopes ($1.34 \times 10^5 \pm 1.26 \times 10^5$ Bq/kg), followed by coniferous forest > deciduous forest > paddy. The ^{134}Cs/^{137}Cs ratio was 0.94 ± 0.11, which is in agreement with that released from FDNPP, indicating that these cesium isotopes originated primarily from the accident. Plutonium-239,240 concentration in the paddy soil column showed a relatively homogeneous distribution with depth (Fig. 4a), similar to that of OC, total I, ^{134}Cs, and ^{137}Cs (Fig. 2a and f, Table 1), most likely due to plowing activity of the top (<15 cm) layer. Plutonium-239,240 concentration decreased with depth in both types of forest soil (Fig. 4a), similar to the trends of ^{134}Cs and ^{137}Cs. Release of ^{239,240}Pu from the FDNPP accident and subsequent deposition at the study sites was quite small, as ^{239,240}Pu activities of the surface soils ranged from 0.02 to 1.31 Bq/kg, which is well within the background range (0.15–4.31 Bq/kg) observed in Japanese soils before the accident (Zheng et al., 2013, 2012). Ratios of ^{240}Pu/^{239}Pu from selected soil samples are displayed in Table 1. The ^{240}Pu/^{239}Pu ratio determined for the litter layer (0.34 ± 0.02) was significantly higher than those typically assigned to global fallout (0.18 ± 0.01) (Zheng et al., 2013) but were closely aligned with the Pu isotopic composition in the damaged cores (0.323–0.330) (Zheng et al., 2012). There are several studies that report similar Pu isotopic ratios in surface vegetation (0.38 ± 0.05) (Schneider et al., 2013) and litter samples (0.30–0.33) (Zheng et al., 2012) collected within the vicinity of the FDNPP. In contrast to the elevated ^{240}Pu/^{239}Pu ratios found in vegetative matter, ^{240}Pu/^{239}Pu in the top surface soils of the coniferous and deciduous forests at our study site were 0.16 ± 0.06 and 0.18 ± 0.01, respectively (Table 1), very close to global fallout ratios. In all, these results indicate that most of the ^{239,240}Pu we measured in this study was not Fukushima-derived and the input of Pu isotopes from the FDNPP accident into soils at the study site was small in terms of total radioactivity, likely causing no significant increase in the environmental ^{239,240}Pu inventory. However, it was sufficient to significantly alter the ^{240}Pu/^{239}Pu ratio in surface vegetation and the litter layer. An estimated release of 0.002% of the overall Pu inventory (14.14×10^{15} Bq in units 1 and 3, Nishihara et al. (2012)) was calculated by Schwantes et al. (2012), and a lower release of 0.00002% was estimated by Zheng et al. (2013) (Zheng et al., 2013, 2012). The FDNPP-derived Pu signal reported by Zheng et al., 2012 was confined to the litter layer in samples collected in May 2011 (Zheng et al., 2012). Our results indicate that the Fukushima-derived Pu signal still has not reached the underlying surface soil as of the March 2014 sampling date. This is in contrast to the distributions of ^{137}Cs and ^{134}Cs, both of which have migrated to at least a depth of 15–22 cm below the soil surface (Table 1). This depth distribution difference, together with the surface distribution difference (see above), suggests that Fukushima-derived Cs and Pu might probably not follow the same deposition and migration mechanisms and patterns. Thus, albeit the existing debate about the released forms of Cs and Pu (Niimura et al., 2015), Cs may eventually sorb to layer-type silicates by forming outer- or inner–sphere complexes (Bostick et al., 2002) in the soil environment, whereas Pu of Fukushima origin has thus far been shown to be mostly associated with litter or plant organic matter. Our results agree with those of Schneider et al. (2013) and confirm that ^{137}Cs is not an adequate environmental proxy for FDNPP released Pu.

The important role of organic matter in affecting ^{239,240}Pu behavior was further supported by a strong positive correlation between its concentration and soil OC contents ($R = 0.72$, $p < 0.001$), as well as a correlation between its concentration and soil nitrogen content ($R = 0.72$, $p < 0.001$) (Fig. 4b, c). Similar

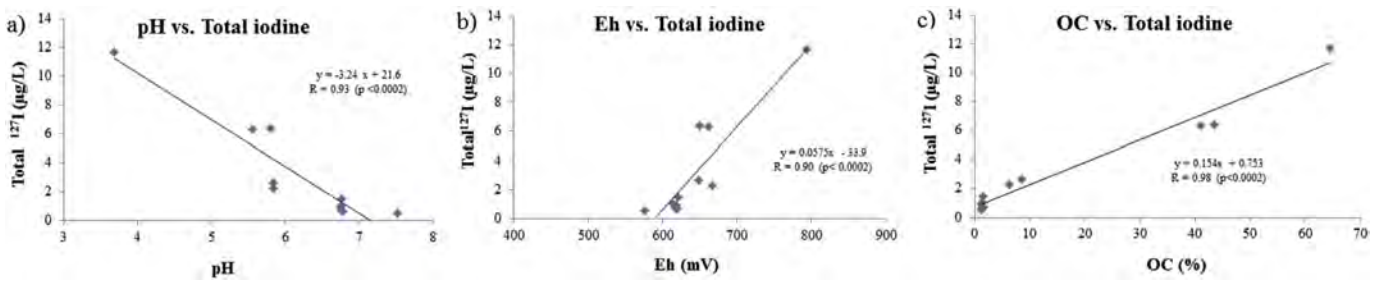

Fig. 3. Correlation relationships between total ^{127}I (μg/L) and a) pH, b) Eh, c) organic carbon (OC) measured from surface and deposition waters (Table 2).

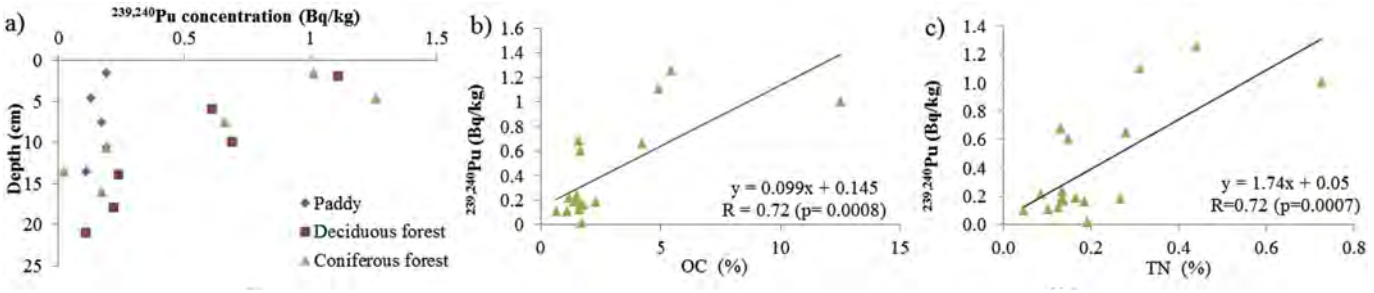

Fig. 4. a) Depth profile of ^{239,240}Pu (Bq/kg) in paddy, deciduous and coniferous forest soil; correlations between ^{239,240}Pu activity concentration (Bq/kg) and b) organic carbon (%, wt); c) total soil nitrogen content (%, wt).

correlation trends were also found in wetland soil samples collected from Savannah River Site (SRS), which was contaminated by Pu isotopes due to nuclear material production and disposal activities (Xu, C. et al., 2015). With the help of multi-NMR techniques and other methods, Xu et al. (2008) reports that mobile Pu, at sub-pM concentrations, in the surface soil at Rocky Flats Environmental Technology Site (RFETS), was complexed by hydroxamate siderophore functionalities (R–CO–NR′-OH) present in colloidal macromolecules composed of cutin-derived soil degradation products as the backbone cross-linked to hydrophilic moieties (e.g., polysaccharides). Recent studies by the same author Xu, C. et al. (2015); confirmed the presence of hydroxamate siderophores in the particulate fractions of wetland soils from SRS, using electrospray ionization (ESI) combined with Fourier-transform ion cyclotron resonance mass spectrometry (FTICRMS). Though no further in-depth characterization of these Pu-associated organic compounds in the Fukushima Prefecture area was pursued, it is likely that hydroxamate siderophore complexing agents are ubiquitous and present in the particulate fraction of soils and sediments in natural environments. Hydroxamate siderophores, present as individual low-molecular-weight compounds, have been detected and are well-studied in dissolved and absorbed fractions of soil aggregates (Ahmed and Holmström, 2014; Essén et al., 2006; Powell et al., 1980, 1983). However, only a few studies so far have reported their presence as high-molecular-weight compounds (>1000 Da) in the colloidal or particulate fractions of SOM (Xu, C. et al., 2015; Xu et al., 2008). It is not clear how these hydroxamate siderophore moieties, initially produced by bacteria or fungi as low-molecular-weight compounds, to solubilize Fe from mineral phases thus to provide bioavailable Fe (III) for microbes and plants, end up part of colloidal or particulate SOM. A possible explanation is that HS functional groups are incorporated into high molecular macromolecules through radical facilitated re-polymerization or cyclization reactions, aided by enzymatically regulated superoxide and hydroxyl radicals (Waggoner et al., 2015), a process suggested for the “imbedding” or crosslinking of lignin in the hemicellulose matrix (Wershaw, 1993).

4. Conclusions

^{127}I, ^{239,240}Pu, ^{134}Cs, and ^{137}Cs all show distinct distributions in vertical profiles or surface soils with different land uses, e.g., urban, paddy, deciduous and coniferous. Our results indicate that ^{137}Cs is not a dependable geochemical proxy for ^{239,240}Pu, or radioiodine in the long-term. ^{127}I concentrations of all surficial soils, regardless of land use type, as well as those of surface water and various rainfall samples, were correlated with organic matter contents, suggesting that natural organic matter is a critical factor affecting iodine biogeochemical behavior. Further, throughfall and stemfall rainwater was not only more enriched in total organic carbon and iodine, but also exclusively consisted of organo-iodine, after it was intercepted by the deciduous or coniferous forest leaves and stems. While Eh and pH also correlated with iodine distribution, the correlation likely only exists within the same type of land use (e.g., urban soil). Although stable iodine (^{127}I) and radioactive iodine (^{131}I and ^{129}I) have completely different sources in that the latter was mostly from atmospheric deposition, resolving the soil properties (Eh, pH and NOM, etc.), which affect stable iodine distribution and might actually exert more controls on radioactive iodine, is important for long-term prediction of the behavior and fate of radioactive iodine.

Absolute ^{239,240}Pu activities in the soil are generally still in the global fallout range before the FDNPP accident. However, an abnormally high ^{240}Pu/^{239}Pu ratio, indicative of FDNPP origin, was found to be confined to litter layers on the soil surface three years after the occurrence of the accident. Plutonium-239,240 activities were significantly correlated to soil OC and nitrogen contents, suggesting ^{239,240}Pu was likely complexed to nitrogen-containing SOM. Further characterization of the specific SOM moieties that are responsible for immobilizing I and Pu, respectively, in Fukushima Prefecture soils would provide fundamental insight serving as a basis for post-accident remediation action plans and future reactor placements.

Acknowledgement

This work was funded by the U.S. Department of Energy (DOE) Office of Science – Subsurface Biogeochemistry Research program (ER65222-1038426-0017532), DOE SBR grant #DE-ER64567-1031562-0014364, DOE SBR award # DE–SC0014152, and DOE contract DE-AD09-96SR18500. Yuko Sugiyama was supported by JSPS Bilateral Joint Research Projects with USA and Grants-in-Aid for Scientific Research #24248027. Nobuhito Ohte was partly supported by a grant for River Management Research (FY2014, 2015) from the River Foundation (Kasen Zaidan, Japan). We really appreciate the Associate Editor Prof. Dr. Shun-ichi Hisamatsu and two anonymous reviewers for their constructive comments that have greatly improved the manuscript.

Appendix A. Supplementary data

Supplementary data related to this article can be found at http://dx.doi.org/10.1016/j.jenvrad.2015.12.022.

References

Ahmed, E., Holmström, S.J.M., 2014. The effect of soil horizon and mineral type on the distribution of siderophores in soil. Geochim. Cosmochim. Acta 131, 184–195.
Ashworth, D.J., 2009. Transfers of iodine in the Soil–Plant–Air system: solid–Liquid partitioning, migration, plant uptake and volatilization (Chapter 11). In:

Watson, E.b.R.P.N.B. (Ed.), Comprehensive Handbook of Iodine. Academic Press, San Diego, pp. 107–118.
ATSDR, 2004. Toxicological Profile for iodine. Agency for Toxic Substances and Disease Registry. U.S. Department of Health and Human Services, Public Health Service, Atlanta, GA.
Baker, A.R., Tunnicliffe, C., Jickells, T.D., 2001. Iodine speciation and deposition fluxes from the marine atmosphere. J. Geophys. Res. Atmos 106, 28743–28749.
Bergkvist, B.O., Folkeson, L., 1992. Soil acidification and element fluxes of a Fagus sylvatica forest as influenced by simulated nitrogen deposition. Water Air Soil Pollut. 65, 111–133.
Bischoff, S., Schwarz, M.T., Siemens, J., Thieme, L., Wilcke, W., Michalzik, B., 2015. Properties of dissolved and total organic matter in throughfall, stemflow and forest floor leachate of central european forests. Biogeosciences 12, 2695–2706.
Bostick, B.C., Vairavamurthy, M.A., Karthikeyan, K.G., Chorover, J., 2002. Cesium adsorption on clay minerals: an EXAFS spectroscopic investigation. Environ. Sci. Technol. 36, 2670–2676.
Campos, M.L.A.M., Nightingale, P.D., Jickells, T.D., 1996. A comparison of methyl iodide emissions from seawater and wet depositional fluxes of iodine over the southern North Sea. Tellus B 48, 106–114.
Chino, M., Nakayama, H., Nagai, H., Terada, H., Katata, G., Yamazawa, H., 2011. Preliminary estimation of release amounts of 131I and 137Cs accidentally Discharged from the fukushima Daiichi nuclear power plant into the atmosphere. J. Nucl. Sci. Technol. 48, 1129–1134.
Ciglasch, H., Lilienfein, J., Kaiser, K., Wilcke, W., 2004. Dissolved organic matter under native Cerrado and pinus caribaea plantations in the brazilian savanna. Biogeochemistry 67, 157–182.
Dai, J.L., Zhang, M., Hu, Q.H., Huang, Y.Z., Wang, R.Q., Zhu, Y.G., 2009. Adsorption and desorption of iodine by various Chinese soils: II. Iodide and iodate. Geoderma 153, 130–135.
Endo, I., Ohte, N., Iseda, K., Tanoi, K., Hirose, A., Kobayashi, N.I., Murakami, M., Tokuchi, N., Ohashi, M., 2015. Estimation of radioactive 137-cesium transportation by litterfall, stemflow and throughfall in the forests of Fukushima. J. Environ. Radioact. 149, 176–185.
Essén, S., Bylund, D., Holmström, S.M., Moberg, M., Lundström, U., 2006. Quantification of hydroxamate siderophores in soil solutions of podzolic soil profiles in Sweden. Biometals 19, 269–282.
Gilfedder, B.S., Petri, M., Biester, H., 2007. Iodine speciation in rain and snow: Implications for the atmospheric iodine sink. J. Geophys. Res. Atmos. 112, D07301.
Guo, J.-f., Yang, Y.-s., Chen, G.-s., Lin, P., 2005. Dissolved organic carbon and nitrogen in precipitation, throughfall and stemflow fromSchima superba andCunninghamia lanceolata plantations in subtropical China. J. For. Res. 16, 19–22.
Hou, X., Aldahan, A., Nielsen, S.P., Possnert, G., 2009. Time series of 129I and 127I speciation in precipitation from Denmark. Environ. Sci. Technol. 43, 6522–6528.
Hou, X.L., Dahlgaard, H., Nielsen, S.P., 2001. Chemical speciation analysis of I-129 in seawater and a preliminary investigation to use it as a tracer for geochemical cycle study of stable iodine. Mar. Chem. 74, 145–155.
Hou, X.L., Povinec, P.P., Zhang, L.Y., Shi, K.L., Biddulph, D., Chang, C.C., Fan, Y.K., Golser, R., Hou, Y.K., Jeskovsky, M., Jull, A.J.T., Liu, Q., Luo, M.Y., Steier, P., Zhou, W.J., 2013. Iodine-129 in seawater offshore fukushima: distribution, inorganic speciation, sources, and budget. Environ. Sci. Technol. 47, 3091–3098.
Hu, Q.H., Moran, J.E., Blackwood, V., 2007. Geochemical cycling of iodine species in soils. In: Preedy, V.R.B., Gerard, N., Watson, Ronald Ross (Eds.), Comprehensive Handbook of Iodine: Nutritional, Biochemical, Pathological and Therapeutic Aspects. Elsevier Inc, Oxford, pp. 93–105.
Hu, Q.H., Zhao, P.H., Moran, J.E., Seaman, J.C., 2005. Sorption and transport of iodine species in sediments from the Savannah river and Hanford Sites. J. Contam. Hydrol. 78, 185–205.
Kaplan, D.I., Brinkmeyer, R., Denham, M.E., Noonkester, J.V., Roberts, K.A., Schwehr, K.A., Vangelas, K.M., Yeager, C.M., Zhang, S., Santschi, P.H., 2010. Groundwater Iodine-129 speciation and its causes for release from a subsurface burial basin. Geochim. Cosmochim. Acta 74. A495–A495.
Kaplan, D.I., Denham, M.E., Zhang, S., Yeager, C., Xu, C., Schwehr, K.A., Li, H.P., Ho, Y.F., Wellman, D., Santschi, P.H., 2014a. Radioiodine biogeochemistry and prevalence in groundwater. Crit. Rev. Environ. Sci. Technol. 44, 2287–2337.
Kaplan, D.I., Roberts, K.A., Schwehr, K.A., Lilley, M.S., Brinkmeyer, R., Denham, M.E., Diprete, D., Li, H.P., Powell, B.A., Xu, C., Yeager, C.M., Zhang, S.J., Santschi, P.H., 2011. Evaluation of a radioiodine plume increasing in concentration at the Savannah river Site. Environ. Sci. Technol. 45, 489–495.
Kaplan, D.I., Zhang, S., Roberts, K.A., Schwehr, K., Xu, C., Creeley, D., Ho, Y.-F., Li, H.-P., Yeager, C.M., Santschi, P.H., 2014b. Radioiodine concentrated in a wetland. J. Environ. Radioact. 131, 57–61.
Kato, H., Onda, Y., Teramage, M., 2012. Depth distribution of 137Cs, 134Cs, and 131I in soil profile after Fukushima Dai-ichi Nuclear power plant Accident. J. Environ. Radioact. 111, 59–64.
Kitamura, A., Yamaguchi, M., Kurikami, H., Yui, M., Onishi, Y., 2014. Predicting sediment and cesium-137 discharge from catchments in eastern Fukushima. Anthropocene 5, 22–31.
Kodama, S., Takahashi, Y., Okumura, K., Uruga, T., 2006. Speciation of iodine in solid environmental samples by iodine K-edge XANES: application to soils and ferromanganese oxides. Sci. Total Environ. 363, 275–284.
Kozai, N., Ohnuki, T., Iwatsuki, T., 2013. Characterization of saline groundwater at Horonobe, Hokkaido, Japan by SEC-UV-ICP-MS: speciation of uranium and iodine. Water Res. 47, 1570–1584.
Lee, M.H., Park, J.H., Oh, S.Y., Ahn, H.J., Lee, C.H., Song, K., Lee, M.S., 2011. Determination of Pu and U isotopes in safeguard swipe sample with extraction chromatographic techniques. Talanta 86, 99–102.
Lv, M.-K., Xie, J.-S., Jiang, M.-H., Luo, S.-J., Zeng, S.-J., Ji, S.-R., Wan, J.-J., Yang, Y.-S., 2014. Comparison on concentrations and quality of dissolved organic matter in throughfall and stemflow in a secondary forest of *Castanopsis carlesii* and *Cunninghamia lanceolata* plantation. Chin. J. Appl. Ecol. 25, 2201–2208.
Matsuda, N., Mikami, S., Shimoura, S., Takahashi, J., Nakano, M., Shimada, K., Uno, K., Hagiwara, S., Saito, K., 2015. Depth profiles of radioactive cesium in soil using a scraper plate over a wide area surrounding the Fukushima Dai-ichi Nuclear power Plant, Japan. J. Environ. Radioact. 139, 427–434.
Meybeck, M., 1982. Carbon, nitrogen and phosphorus transport by world rivers. Am. J. Sci. 282, 401–450.
Meybeck, M., 1988. How to Establish and Use World Budgets of Riverine Materials. Kluwer Academic Publishers, Dordrecht.
Michalzik, B., Kalbitz, K., Park, J.H., Solinger, S., Matzner, E., 2001. Fluxes and concentrations of dissolved organic carbon and nitrogen – a synthesis for temperate forests. Biogeochemistry 52, 173–205.
Montelius, M., Thiry, Y., Marang, L., Ranger, J., Cornelis, J.T., Svensson, T., Bastviken, D., 2015. Experimental evidence of large changes in terrestrial chlorine cycling following altered tree species composition. Environ. Sci. Technol. 49, 4921–4928.
Morgenstern, A., Apostolidis, C., Carlos-Marquez, R., Mayer, K., Molinet, R., 2002. Single-column extraction chromatographic separation of U, Pu, Np and Am. Radiochim. Acta 90, 81–85.
Neal, C., Smith, C.J., Walls, J., Billingham, P., Hill, S., Neal, M., 1990. Comments on the hydrochemical regulation of the halogen elements in rainfall, stemflow, throughfall and stream waters at an acidic Forested area in Mid-Wales. Sci. Total Environ. 91, 1–11.
Niimura, N., Kikuchi, K., Tuyen, N.D., Komatsuzaki, M., Motohashi, Y., 2015. Physical properties, structure, and shape of radioactive Cs from the Fukushima Daiichi Nuclear power plant accident derived from soil, bamboo and shiitake mushroom measurements. J. Environ. Radioact. 139, 234–239.
Nishihara, K., Iwamoto, H., Suyama, K., 2012. Estimation of Fuel Compositions in Fukushima-daiichi Nuclear Power Plant. Japan Atomic Energy Agency, Tokai, Japan.
Povinec, P.P., Aoyama, M., Biddulph, D., Breier, R., Buesseler, K., Chang, C.C., Golser, R., Hou, X.L., Jeskovsky, M., Jull, A.J.T., Kaizer, J., Nakano, M., Nies, H., Palcsu, L., Papp, L., Pham, M.K., Steier, P., Zhang, L.Y., 2013. Cesium, iodine and tritium in NW Pacific waters – a comparison of the Fukushima impact with global fallout. Biogeosciences 10, 5481–5496.
Powell, P.E., Cline, G.R., Reid, C.P.P., Szaniszlo, P.J., 1980. Occurrence of hydroxamate siderophore iron Chelators in soils. Nature 287, 833–834.
Powell, P.E., Szaniszlo, P.J., Reid, C.P.P., 1983. Confirmation of occurrence of hydroxamate siderophores in soil by a Novel Escherichia-Coli bioassay. Appl. Environ. Microbiol. 46, 1080–1083.
Qualls, R.G., Haines, B.L., Swank, W.T., 1991. Fluxes of dissolved organic Nutrients and humic substances in a deciduous Forest. Ecology 72, 254–266.
Ryba, S.A., Burgess, R.M., 2002. Effects of sample preparation on the measurement of organic carbon, hydrogen, nitrogen, sulfur, and oxygen concentrations in marine sediments. Chemosphere 48, 139–147.
Savannah River Nuclear Solutions, 2013. Savannah River Site Environmental Report for 2013. Savannah River Site, Aiken SC, p. 29808.
Schneider, S., Walther, C., Bister, S., Schauer, V., Christl, M., Synal, H.A., Shozugawa, K., Steinhauser, G., 2013. Plutonium release from Fukushima Daiichi fosters the need for more detailed investigations. Sci. Rep. 3. Uk.
Schwantes, J.M., Orton, C.R., Clark, R.A., 2012. Analysis of a nuclear accident: Fission and activation product releases from the fukushima Daiichi nuclear Facility as remote indicators of source identification, extent of release, and state of damaged spent nuclear fuel. Environ. Sci. Technol. 46, 8621–8627.
Schwehr, K.A., Santschi, P.H., Kaplan, D.I., Yeager, C.M., Brinkmeyer, R., 2009. Organo-iodine Formation in soils and aquifer sediments at ambient concentrations. Environ. Sci. Technol. 43, 7258–7264.
Shetaya, W.H., Young, S.D., Watts, M.J., Ander, E.L., Bailey, E.H., 2012. Iodine dynamics in soils. Geochim. Cosmochim. Acta 77, 457–473.
Shimamoto, Y., Takahashi, Y., 2008a. Iodine Speciation in the Soil-water Systems Using XANES and HPLC-ICP-MS. Geophysical Research Abstracts. EGU2008-A-06989.
Shimamoto, Y.S., Takahashi, Y., 2008b. Superiority of K-edge XANES over L-III-edge XANES in the speciation of iodine in natural soils. Anal. Sci. 24, 405–409.
Shimamoto, Y.S., Takahashi, Y., Terada, Y., 2011. Formation of organic iodine supplied as iodide in a soil-water system in Chiba, Japan. Environ. Sci. Technol. 45, 2086–2092.
Shinonaga, T., Steier, P., Lagos, M., Ohkura, T., 2014. Airborne plutonium and non-natural uranium from the fukushima DNPP found at 120 km Distance a few Days after reactor hydrogen explosions. Environ. Sci. Technol. 48, 3808–3814.
Takata, H., Zheng, J., Tagami, K., Aono, T., Fujita, K., Yamasaki, S., Tsuchiya, N., Uchida, S., 2013. Distribution coefficients (K (d)) of stable iodine in estuarine and coastal regions, Japan, and their relationship to salinity and organic carbon in sediments. Environ. Monit. Assess. 185, 3645–3658.
Takeda, A., Tsukada, H., Takahashi, M., Takaku, Y., Hisamatsu, S., 2015. Changes in the chemical form of exogenous iodine in forest soils and their extracts. Radiat. Prot. Dosim 167, 181–186.
Truesdale, V.W., Jones, S.D., 1996. The variation of iodate and total iodine in some UK rainwaters during 1980–1981. J. Hydrol. 179, 67–86.
Wada, K., 1985. The distinctive properties of Andosols. In: Stewart, B.A. (Ed.),

Advances in Soil Science. Springer-Verlag New York, Inc., New York, pp. 173–229.
Waggoner, D.C., Chen, H., Willoughby, A.S., Hatcher, P.G., 2015. Formation of black carbon-like and alicyclic aliphatic compounds by hydroxyl radical initiated degradation of lignin. Org. Geochem. 82, 69–76.
Wershaw, R.L., 1993. Model for humus in soils and sediments. Environ. Sci. Technol. 27, 814–816.
Xu, C., Chen, H., Sugiyama, Y., Zhang, S., Li, H.-P., Ho, Y.-F., Chuang, C.-y, Schwehr, K.A., Kaplan, D.I., Yeager, C., Roberts, K.A., Hatcher, P.G., Santschi, P.H., 2013. Novel molecular-level evidence of iodine binding to natural organic matter from Fourier transform ion cyclotron resonance mass spectrometry. Sci. Total Environ. 449, 244–252.
Xu, C., Miller, E.J., Zhang, S.J., Li, H.P., Ho, Y.F., Schwehr, K.A., Kaplan, D.I., Otosaka, S., Roberts, K.A., Brinkmeyer, R., Yeager, C.M., Santschi, P.H., 2011a. Sequestration and remobilization of radioiodine (I-129) by soil organic matter and possible Consequences of the remedial action at Savannah river site. Environ. Sci. Technol. 45, 9975–9983.
Xu, C., Zhang, S., kaplan, D., Ho, Y.-F., Schwehr, K., Roberts, K.A., Chen, H., DiDonato, N., Athon, M., Hatcher, P., Santschi, P., 2015. Evidence for hydroxamate siderophores and other N-containing organic compounds controlling 239,240Pu immobilization and re-mobilization in a wetland sediment. Environ. Sci. Technol 49, 11458–11467.
Xu, C., Santschi, P.H., Zhong, J.Y., Hatcher, P.G., Francis, A.J., Dodge, C.J., Roberts, K.A., Hung, C.C., Honeyman, B.D., 2008. Colloidal cutin-like substances cross-linked to siderophore decomposition products mobilizing plutonium from contaminated soils. Environ. Sci. Technol. 42, 8211–8217.
Xu, C., Zhang, S., Ho, Y.-F., Miller, E.J., Roberts, K.A., Li, H.-P., Schwehr, K.A., Otosaka, S., Kaplan, D.I., Brinkmeyer, R., Yeager, C.M., Santschi, P.H., 2011b. Is soil natural organic matter a sink or source for mobile radioiodine (129I) at the Savannah river Site? Geochim. Cosmochim. Acta 75, 5716–5735.
Xu, C., Zhong, J.Y., Hatcher, P.G., Zhang, S.J., Li, H.P., Ho, Y.F., Schwehr, K.A., Kaplan, D.I., Roberts, K.A., Brinkmeyer, R., Yeager, C.M., Santschi, P.H., 2012. Molecular environment of stable iodine and radioiodine (I-129) in natural organic matter: evidence inferred from NMR and binding experiments at environmentally relevant concentrations. Geochimica Cosmochim. Acta 97, 166–182.
Xu, S., Freeman, S.P.H.T., Hou, X., Watanabe, A., Yamaguchi, K., Zhang, L., 2013. Iodine isotopes in precipitation: temporal responses to 129I emissions from the fukushima nuclear accident. Environ. Sci. Technol. 47, 10851–10859.
Xu, S., Zhang, L., Freeman, S.P.H.T., Hou, X., Shibata, Y., Sanderson, D., Cresswell, A., Doi, T., Tanaka, A., 2015. Speciation of radiocesium and radioiodine in aerosols from Tsukuba after the fukushima nuclear accident. Environ. Sci. Technol. 49, 1017–1024.
Yamada, H., Kiriyama, T., Onagawa, Y., Hisamori, I., Miyazaki, C., Yonebayashi, K., 1999. Speciation of iodine in soils. Soil Sci. Plant Nutr. 45, 563–568.
Yamaguchi, N., Nakano, M., Takamatsu, R., Tanida, H., 2010. Inorganic iodine incorporation into soil organic matter: evidence from iodine K-edge X-ray absorption near-edge structure. J. Environ. Radioact. 101, 451–457.
Yamamoto, M., Sakaguchi, A., Ochiai, S., Takada, T., Hamataka, K., Murakami, T., Nagao, S., 2014. Isotopic Pu, am and Cm signatures in environmental samples contaminated by the Fukushima Dai-ichi Nuclear power plant accident. J. Environ. Radioact. 132, 31–46.
Yamamoto, M., Takada, T., Nagao, S., Koike, T., Shimada, K., Hoshi, M., Zhumadilov, K., Shima, T., Fukuoka, M., Imanaka, T., Endo, S., Sakaguchi, A., Kimura, S., 2012. An early survey of the radioactive contamination of soil due to the Fukushima Dai-ichi Nuclear power plant accident, with emphasis on plutonium analysis. Geochem J. 46, 341–353.
Yasunari, T.J., Stohl, A., Hayano, R.S., Burkhart, J.F., Eckhardt, S., Yasunari, T., 2011. Cesium-137 deposition and contamination of Japanese soils due to the Fukushima nuclear accident. Proc. Natl. Acad. Sci. 108, 19530–19534.
Zhang, S., Du, J., Xu, C., Schwehr, K.A., Ho, Y.F., Li, H.P., Roberts, K.A., Kaplan, D.I., Brinkmeyer, R., Yeager, C.M., Chang, H.S., Santschi, P.H., 2011. Concentration-dependent mobility, retardation, and speciation of iodine in surface sediment from the Savannah river site. Environ. Sci. Technol. 45, 5543–5549.
Zhang, S., Ho, Y.-F., Creeley, D., Roberts, K.A., Xu, C., Li, H.-P., Schwehr, K.A., Kaplan, D.I., Yeager, C.M., Santschi, P.H., 2014. Temporal variation of iodine concentration and speciation (127I and 129I) in wetland groundwater from the Savannah river site, USA. Environ. Sci. Technol. 48, 11218–11226.
Zhang, S., Schwehr, K.A., Ho, Y.F., Xu, C., Roberts, K.A., Kaplan, D.I., Brinkmeyer, R., Yeager, C.M., Santschi, P.H., 2010. A Novel approach for the simultaneous determination of iodide, iodate and organo-iodide for I-127 and I-129 in environmental samples using Gas Chromatography-mass spectrometry. Environ. Sci. Technol. 44, 9042–9048.
Zhang, S., Xu, C., Creeley, D., Ho, Y.-F., Li, H.-P., Grandbois, R., Schwehr, K.A., Kaplan, D.I., Yeager, C.M., Wellman, D., Santschi, P.H., 2013. Iodine-129 and Iodine-127 speciation in groundwater at the Hanford site, U.S.: Iodate incorporation into Calcite. Environ. Sci. Technol. 47, 9635–9642.
Zheng, J., Tagami, K., Uchida, S., 2013. Release of plutonium isotopes into the environment from the fukushima Daiichi nuclear power plant accident: what is known and what Needs to Be known. Environ. Sci. Technol. 47, 9584–9595.
Zheng, J., Tagami, K., Watanabe, Y., Uchida, S., Aono, T., Ishii, N., Yoshida, S., Kubota, Y., Fuma, S., Ihara, S., 2012. Isotopic evidence of plutonium release into the environment from the Fukushima DNPP accident. Sci. Rep. 2.